Analyst

Accepted Manuscript

This article can be cited before page numbers have been issued, to do this please use: J. N. S. N.S. Sboto and C. Gill, *Analyst*, 2025, DOI: 10.1039/D5AN01073J.

ROYAL SOCIETY OF CHEMISTRY

rsc.li/analyst

View Article Online
DOI: 10.1039/D5AN01073J

Computational and Design of Experiment Strategies to Improve Differentiation and Quantitation of Trace-Level Cannabinoids by Copper Cationization Paper Spray Mass Spectrometry

Jindar N. S. Sboto[1, 2], and Chris G. Gill[1, 2, 3, 4*]

[1] Centre for Health and Environmental Mass Spectrometry (CHEMS), Chemistry Department, Vancouver Island University, Nanaimo, BC, Canada, V9R 5S5
[2] Chemistry Department, University of Victoria, Victoria, BC, Canada, V8P 5C2
[3] Canadian Institute for Substance Use Research (CISUR), University of Victoria, Victoria, BC, Canada V8W 2Y2
[4] Department of Occupational and Environmental Health Sciences, University of Washington, Seattle, WA, United States, 98195-1618

***Address correspondence to:**

Professor Chris G. Gill, Ph.D., P. Chem.
Co-Director, Center for Health and Environmental Mass Spectrometry (CHEMS)
Chemistry Department
Vancouver Island University
900 Fifth Street, Nanaimo, BC, Canada, V9R 5S5

Ph: 250-753-3245
chris.gill@viu.ca

View Article Online
DOI: 10.1039/D5AN01073J

ABSTRACT

The medicinal and recreational use of cannabis products is quickly rising from increased worldwide legalization and decriminalization. Despite this, current analytical methods have compromises when analyzing common isobaric cannabinoids, such as cannabidiol (CBD) or (-)-trans-Δ9-tetrahydrocannabinol (THC). We report on the use of computational chemistry, combined with design of experiment (DoE), to optimize and develop a paper spray mass spectrometry (PS-MS) method with on-paper cationization to simplify workflow for trace level differentiation and quantitation of THC and CBD. Computational methods allowed for pre-screening of candidate metal ions prior to experimental measurements, with promising candidates then being evaluated by electrospray ionization high resolution mass spectrometry (ESI-HRMS). A direct mass spectrometry method using copper cationization with PS-MS was then developed and optimized using DoE. Copper cationization with both ESI and PS-MS tandem mass spectrometry demonstrated the best CBD/THC selectivity and sensitivity, with 1% interference between CBD and THC copper adduct product ions with ESI. DoE results increased the analytical performance of the PS-MS method for quantifying cannabinoids in methanol, acetonitrile/water, and saliva matrices. Methanolic detection limits were 10 ng/mL for CBD and 20 ng/mL for THC by PS-MS allowing rapid (one-minute measurement), direct mass spectrometry differentiation, whereas detection limits in both saliva and acetonitrile/water matrices were <2 ng/mL for THC and CBD. This work illustrates the advantages of using DoE and computational chemistry to develop PS-MS and ESI methods for the rapid differentiation and quantitation of isobaric cannabinoids.

KEYWORDS

Paper Spray Mass Spectrometry, On-paper Cationization, Cannabinoids, THC, CBD, Copper Adducts, Design of Experiment, Density Functional Theory

View Article Online
DOI: 10.1039/D5AN01073J

INTRODUCTION

The rise of cannabis product use worldwide[1] has led to increased need for analytical techniques capable of rapidly differentiating and quantifying cannabinoids at low ng/mL levels. Cannabinoids, the active medicinal and psychoactive compounds found in the cannabis plant, share many common isomers with the molecular formula $C_{21}H_{30}O_2$. The two most used and studied cannabinoids are (-)-trans-Δ9-tetrahydrocannabinol (THC) and cannabidiol (CBD), which are isobaric and have similar tandem mass spectrometry (MS/MS) fragmentation, complicating their differentiation by direct mass spectrometry.[2] CBD is typically used for its therapeutic properties, such as decreasing arthritic inflammation, and easing pain.[3] THC is psychoactive, associated with the "high" that is experienced from using cannabis products.[3] Because of this, regulatory bodies impose strict regulations on THC concentrations allowed in therapeutic CBD products, typically <0.3 % THC by dry weight in the European Union.[4] Similarly, the regulatory limit for THC detection in saliva as set by the US Substance Abuse and Mental Health Association (SAMHSA) is 2 ng/mL.[5] With increased global cannabis legalization, a need for testing of impaired drivers has also arisen, with one study finding that driving under the influence of cannabis doubled after its legalization in Canada in 2018.[6] Cannabinoid testing typically relies on either gas or liquid chromatography mass spectrometry methods for regulatory testing, or immunoassay-based techniques for roadside testing.[6,7] This means regulatory testing is often slow and expensive, whereas on-site roadside testing has poor analytical robustness, being on average 38% sensitive, 95% specific, and 73% accurate for cannabinoid presence.[7] Further, cannabinoids have many potentially psychoactive isomers, complicating their quantitation in both commercial products and enforcement purposes.[8] Therefore, rapid, direct methods for the analysis of cannabinoids are necessary to alleviate testing backlogs and improve on-site analysis capabilities.

Paper spray mass spectrometry (PS-MS) is an ambient ionization, direct mass spectrometry approach that is gaining popularity for rapid, quantitative chemical measurements in a wide range of applications.[9–12] Paper spray ionization is similar to electrospray ionization (ESI) in that the ionization efficiency of compounds is dependent on the presence of ionizable moieties, such as carboxylic acids, or amines.[11,13] PS-MS and ESI both struggle with the

View Article Online
DOI: 10.1039/D5AN01073J

measurement of compounds that lack ionizable groups. Attempts to improve detection and quantitation of both synthetic and natural cannabinoids by PS-MS include adding extraction methods prior to quantitation,[14,15] preconcentration using oils,[16] modifying the paper substrate to mitigate matrix effects,[17], or by modifying spray solvents to increase ionization efficiency.[18] Metal ion adducts can be used to enhance ionization efficiency by forming complexes with transition and alkali earth metals.[19,20] For cannabinoids, the use of silver ion (Ag^+) cationization with ESI and PS-MS (termed argentation), has been demonstrated.[19,21] Argentation has increased the PS-MS ionization efficiency and sensitivity of cannabinoids by over 500%, making it possible to quantify cannabinoids in the lower ng/mL range by PS-MS, albeit with incomplete differentiation.[19,21] Unfortunately, argentation has not yet been used for measurements in biofluids, and still has limitations in terms of sensitivity, with current lower limits of detection (LLOD) around 15 ng/mL in cannabis oils.[19,21] Other reactive methods to improve cannabinoid ionization have been explored, such as adding triphenyl phosphine to the argentated cannabinoids to be measured with ESI,[22,23] or by using reactive PS-MS methods employing azo-salts such as Fast Red RC.[24] Additionally, miniaturized mass spectrometers with ambient ionization methods have been used for quantifying synthetic cannabinoids in biofluids,[25,26] providing a potential option for roadside testing. These methods have limitations, such as the lack of differentiation by azo-salt reaction,[24] or being semi-quantitative in the case of triphenyl phosphine complexation.[23] To our knowledge, other metal ion cationization strategies have not yet been explored for ionization enhancement of cannabinoids.

Metal ion selection and optimizing cationization conditions is a tedious process, frequently involving significant trial and error.[27] Computational methods can accelerate this task by screening the utility of candidate metal ions *in silico* prior to mass spectrometry, providing insight into the best metal ions to explore. Calculating the change in Gibbs Energy (ΔG) (Equation 1), allows estimation of thermodynamic favourability for cannabinoid metal complexation.

$$\Delta G = G_{[MCannabinoid]^+} - (G_{Cannabinoid} + G_{M^+}) \qquad \text{Equation 1}$$

View Article Online
DOI: 10.1039/D5AN01073J

Using this approach, pre-screening a wide variety of metal ions in various oxidation states can be accomplished, identifying potential candidates for mass spectrometry applications.

In this work, computational chemistry and design of experiment (DoE)[28] were employed to develop an improved method for differentiating and quantifying trace-level CBD and THC using on-paper copper cationization with PS-MS. Following computational screening, ESI-HRMS was used to evaluate promising candidates, which were subsequently evaluated for analytical performance by ESI with a triple quadrupole mass spectrometer. DoE was used to optimize copper cationization conditions for PS-MS which is sensitive to the concentration of impregnated metal cations. Final optimized quantitative evaluations were conducted using PS-MS/MS with a triple quadrupole mass spectrometer. Using on-paper cationization with PS-MS simplifies the analytical workflow by reducing reagent consumption per measurement and sample preparation steps.[19,21,24] We present a sensitive method for selectively quantifying THC and CBD that meets regulatory sensitivity guidelines.[4,5]

EXPERIMENTAL

Reagents and Materials

HPLC-grade methanol, acetonitrile, and water (<10 ppb total metal content) were purchased from Fisher Scientific (Vancouver, BC, Canada). Human saliva was sourced from anonymous volunteers. Whatman 31ET pointed PS-MS strips (6 mm base, 29 mm from base to tip, 38° tip angle) were obtained courtesy of Thermo Fisher Scientific (San Jose, California, USA). Metal salts (CuCl, LiOAc, $PdCl_2$, $SnCl_2$) were purchased from Sigma Aldrich Chemical Company (Burlington, Massachusetts, USA). Methanolic cannabinoid standards (THC, CBD, CBD-d_9) were purchased from the Cerilliant Chemical Company (Round Rock, Texas, USA). Unless otherwise noted, all solutions, standards, and samples were prepared in 2 mL glass vials with Teflon™ faced septa caps from Fisher Scientific (Mississauga, Ontario, Canada).

Computational Methods

Computations were performed using the Digital Research Alliance of Canada (DRAC) clusters, Graham, and Cedar. The software package employed

View Article Online
DOI: 10.1039/D5AN01073J

was Gaussian 16 revision C.01, using Gaussview 6.1.1 for visualization and modelling.[29,30] Free energies for gas phase and solvated systems were calculated using the ωB97XD functional[31,32] and def2-TZVPPD basis set, with basis sets obtained courtesy of BasisSetExchange.org.[33–39] Two solvated systems, MeOH and H_2O, were investigated using the SMD solvation model included in the Gaussian package. The free energies for metal ions, cannabinoids, and cannabinoid metal adducts were calculated individually in each solvent system. Gibb's energy for solvated systems were calculated using the electronic energy from the SMD calculation, with the thermal free energy correction from the gas phase system.[40] Initial structures were optimized using a HF LanL2DZ level of theory prior to optimization with more computationally expensive methods.[41,42] Input files and output files are openly available in the Vancouver Island University Dataverse (See Associated Content).

ESI High Resolution Mass Spectrometry

To verify computational findings for metal-cannabinoid complexation, 5 µg/mL solutions of each metal salt and 500 ng/mL of either THC or CBD were prepared in HPLC-grade methanol. ESI with a 10 µL/min direct infusion flow rate was used to introduce samples to an Orbitrap mass spectrometer (Exploris 120™, Thermo Fisher Scientific). Spray voltage for each adduct was optimized using Orbitrap Exploris 120™ Tune Application (Version 4.2.362.16, Thermo Fisher Scientific). For full scans, 60 seconds of data were collected. For product ion spectra, HCD cell fragmentation voltage was ramped from 1-40 V in 5 V increments, collecting 15 seconds of data at each voltage. Unless otherwise noted, the most intense copper isotope (^{63}Cu) adduct was used for HRMS characterization and quantitative analyses. HRMS operating conditions are summarized in the Supplementary Information, Table S1. Product *m/z* were assigned using Xcalibur™ Qual Browser (Version 4.5.474.0, Thermo Fisher Scientific), with a 5 ppm mass tolerance cutoff.

ESI Triple Quadrupole Mass Spectrometry

Initial quantitative performance of copper cannabinoid adducts was evaluated using ESI with a 10 µL/min direct infusion flow rate and a triple quadrupole mass spectrometer (TSQ Altis™, Thermo Fisher Scientific). MRM

transitions were optimized using TSQ Altis™ Tune Application (Version 3.4.3268.14, Thermo Fisher Scientific), with ions of highest intensity being used (also confirmed by HRMS). Optimal MRM conditions are given in Table S2. To evaluate interference between THC/CBD MRMs, a series of methanolic standards (0, 5, 10, 25, 100, 250, 500 ng/mL) of either THC or CBD were analyzed by ESI-MS, using 100 ng/mL CBD-d_9 as internal standard (ISTD) for each, since CBD and THC are expected to have similar ionization efficiencies. The measured response was integrated area of cannabinoid divided by integrated area of the internal standard. Unless otherwise noted, data was processed using TraceFinder™ (Clinical LC Version 5.1, Thermo Fisher Scientific) and Microsoft 365 Excel, and standard residuals for calibrations were monitored to ensure no bias from any data point. Instrument parameters for these investigations are given in Table S3.

Paper Spray Mass Spectrometry

PS-MS analysis was performed using a high throughput, commercially available paper spray ion source (VeriSpray™ Paper Spray Ion Source, Thermo Fisher Scientific) and a triple quadrupole mass spectrometer (TSQ Altis™, Thermo Fisher Scientific). Instrument parameters for PS-MS are summarized in Tables S4-S6, with MRM transitions optimized using an in-house constructed PS-MS source (described elsewhere),[43] summarized in Table S7. Based on our unpublished observations, to eliminate any signal suppression effects from MS inlet ion optic charging when using PS-MS, ionization polarity switching was employed. Design of experiment optimized strips (described below) were spotted with 10 µL of sample matrix before drying at 40 °C (VWR Oven Gr Con 2.3CF, VWR International, Radnor, PA, USA) for 10 minutes prior to a rapid one-minute PS-MS analysis using 90/10/0.1 % MeOH/H_2O/Formic acid spray and rewet solvent. To evaluate interference between THC/CBD MRMs, a series of standards in 3:1 acetonitrile/water matrix (0, 5, 10, 25, 100, 250, 500 ng/mL) of either THC or CBD were analyzed by PS-MS, using 100 ng/mL CBD-d_9 as internal standard (ISTD). The measured response was integrated area of cannabinoid divided by integrated area of the internal standard.

View Article Online
DOI: 10.1039/D5AN01073J

Design of Experiment

Design of Experiment (DoE) is an experimental approach to study and assess the influence of experimental factors simultaneously while considering interactions between different factors.[28] DoE was performed using Stat-Ease 360 Software (Version 23.1.7, Stat-Ease Inc., Minneapolis, MN, USA).[44] Randomized central composite designs were used for optimization of copper ion solution concentrations and PS-MS paper strip soak times. For DoE, unmounted PS-MS paper strips were soaked in methanolic CuCl solutions prepared in 2 mL red Safe-Lock™ Eppendorf™ Tubes (Eppendorf Inc., Mississauga, Ontario, Canada), with conditions summarized in Table S8. The strips were subsequently mounted in VeriSpray™ paper spray sample plates (Thermo Fisher Scientific) and air dried at 40 °C for 10 minutes. The prepared strips were spotted with 10 µL of a methanolic 500 ng/mL THC and CBD-d_9 standard and dried at 40 °C for 10 minutes. For measurements in saliva matrix, a simple 3:1 acetonitrile to saliva protein crash was used, vortexing the samples with acetonitrile for 30 seconds (Fisher Digital Vortex, Cat. No. 02215418, Fisher Scientific) at 3000 (arbitrary) speed prior to sample spotting. THC and CBD-d_9 MRMs were monitored as the response for DoE, whereas CBD MRMs were monitored as a control for noise. Response surface diagrams were generated using the software recommended best-fit model, chosen to lower aliasing and increase model fit confidence. Residuals, Cooks Distance, DFFITS, and leverage were monitored to ensure no bias from any single data point. For methanolic samples, optimized conditions were 200 µg/mL CuCl in methanol and 30 min soak time, whereas for saliva matrix samples the optimized conditions were determined to be 600 µg/mL CuCl in methanol and 25 min soak time.

Quantitative PS-MS Evaluation

Using DoE optimized conditions for PS-MS, combined calibration curves for methanolic THC and CBD were obtained (0, 2, 5, 25, 100, 250, 500 ng/mL levels, n = 5 replicates per level). Calibration verifications were performed at 10 ng/mL, 50 ng/mL, and 300 ng/mL (n = 5 replicates per point). Samples were spotted onto dry CuCl impregnated PS-MS paper strips and dried for 10 minutes at 40 °C prior to analysis. The extended drying times employed in the PS-MS studies were used to minimize any variability from residual solvent/moisture,

View Article Online
DOI: 10.1039/D5AN01073J

however this is not typically necessary for PS-MS measurements.[45] The same 3:1 acetonitrile to saliva protein crash employed during DoE was used for the saliva matrix calibrations. Calibration levels were 0, 2, 25, 100, 250, 500, and 1000 ng/mL in saliva prior to the acetonitrile protein crash, with 5 replicates per point and with calibration verifications, using a different source of saliva, performed at 10, 50, and 300 ng/mL. Calibration curves for acetonitrile/water matrix were obtained (0, 0.5, 2, 25, 100, 250, 500, 1000 ng/mL levels, n = 5 replicates per level) using the same paper soak conditions as the saliva matrix, with calibration verifications also performed at the same levels. Copper impregnated paper stability was evaluated by pre-preparing optimized paper substrate, which was stored in a sealed plastic bag with a desiccant packet in the vendor shipping box prior to measurement. At 0, 3h, 6h, 48h, and 72h, the paper strips were loaded with 10 µL of 250 ng/mL THC and CBD acetonitrile/water solution (with ISTD) and measured by the optimized method.

RESULTS AND DISCUSSION

Density Functional Theory Simulations

Eighteen alkali, alkali-earth, and transition metals in various oxidation states were chosen for computational screening (further details regarding computational screening is provided in the supplementary information). The ΔG for complexation with THC and CBD is tabulated in Tables S9-S11, and trends in relative thermodynamic favourability were evaluated. Because Ag(I) cationization is known to increase the ionization efficiency of cannabinoids with ESI and PS-MS, it was used as our 'benchmark' to evaluate adduct formation suitability. For singly charged cation complexes, Au^+ and Cu^+ exhibited greater thermodynamic favourability than Ag^+, which has been previously reported experimentally for alkyne and alkene complexes of the d^{10} centers,[46] whereas Li^+ was slightly less favourable than Ag^+. For doubly charged cation complexes, Sn^{2+}, Pd^{2+}, and Pt^{2+}, showed greater thermodynamic favourability than Ag^+. These results are likely overinflated due to greater electrostatic interactions for 2+ ions. In this work, Pt^{2+} and Au^+ were not investigated further due to lack of availability and cost. The candidate metal cations, Cu^+, Li^+, Pd^{2+}, and Sn^{2+} were chosen for HRMS evaluations.

View Article Online
DOI: 10.1039/D5AN01073J

High Resolution Mass Spectrometry

Copper Adducts. Copper adducts of THC and CBD were observed by ESI-HRMS (Figure 1A). Although Cu^+ was used as the initial source of metal cations in these experiments, the primary adducts formed for both THC and CBD were Cu^{2+} complexes with a (proposed) proton loss from the cannabinoid hydroxyl group yielding an overall 1+ complex. This is likely due to the presence of Cu^{2+} (d^9 center) in solution from the autooxidation of Cu^+ in solution from the presence of O_2,[47] thus electron donation from a deprotonated hydroxyl group allows return to energetically favourable d^{10} configuration. For PS-MS, the most sensitive MRM observed for THC was a Cu^{2+} adduct whereas CBD favoured a Cu^+ adduct. By using a Cu^+ salt, sufficient Cu^+ and Cu^{2+} ions are present to allow simultaneous quantitation. Additionally, hydrated [CuCannabinoid+H_2O-H]$^+$ (*m/z* 394.1561/396.1537) adducts were seen in roughly equal intensity compared to the non hydrated adducts for THC, but not for CBD. We hypothesize that this could be due to free rotation around the ring-ring bond in CBD, which is not possible for THC. CBD can rotate to provide a distorted square planar complex, whereas copper THC complexes may need additional stabilization from H_2O or another ligand (Figure 2). [CuCannabinoid]$^+$ complexes were observed at *m/z* 377.1486 and 379.1519 for ^{63}Cu and ^{65}Cu, however these were far less intense than their Cu^{2+} counterparts [CuCannabinoid-H]$^+$ observed at *m/z* 376.1453/378.1441 (Figure 1A) by ESI-HRMS.

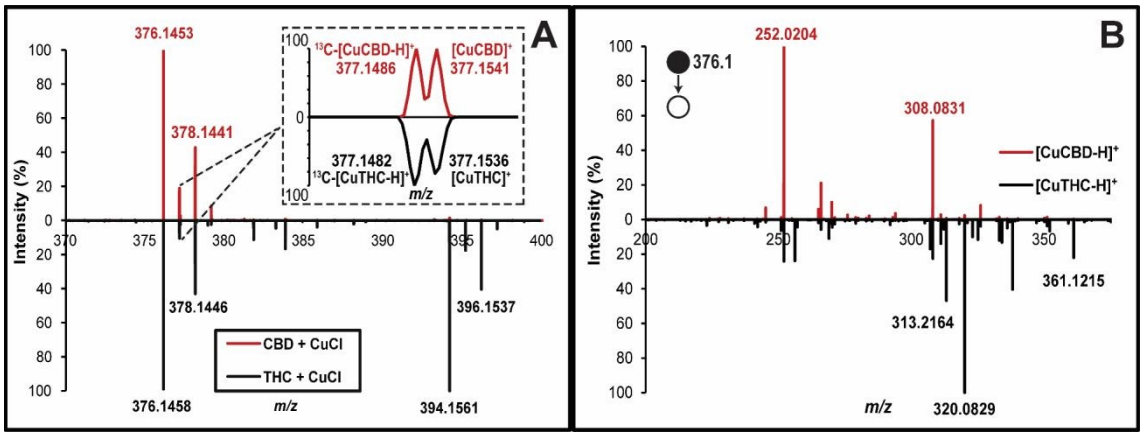

Figure 1. (A) [CuTHC-H]$^+$ adducts were observed at *m/z* 376.1458/378.1446 for complexes with Cu^{2+}, with minor *m/z* 377.1539/379.1519 ions for complexes with

Cu^+. Hydrated adducts were also observed at +18 *m/z* to the corresponding peaks. (B) Product ion spectra for both [CuCannabinoid-H]$^+$ precursors (*m/z* 376.1), with HCD energy at 20 V and Orbitrap resolution of 120 000. Different fragmentation for [CuCBD-H]$^+$ and [CuTHC-H]$^+$ is evident from the product ions, such as *m/z* 361.1215, 320.0829, and 313.2164 for THC, or *m/z* 308.0831 and 252.0204 for CBD.

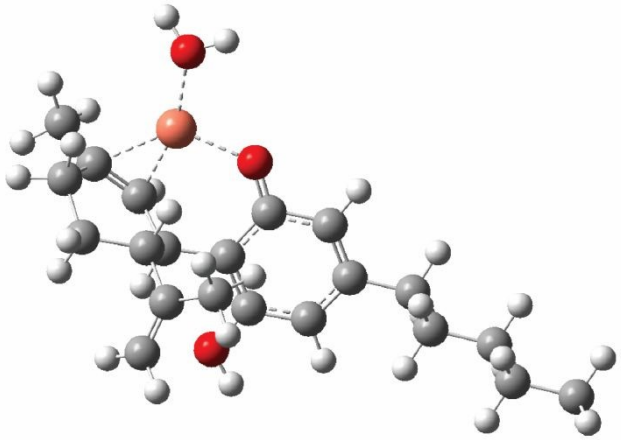

Figure 2. Computational geometry optimized structure for [CuTHC+H_2O-H]$^+$ (ωB97XD/def2-TZVPPD). A distorted square planar structure is observed, consistent with the favourable geometry for the Cu^{2+} ion.

MS/MS differentiation of cannabinoids by [CuTHC-H]$^+$ and [CuCBD-H]$^+$ (Figure 1B) is evident in their HRMS/MS spectra. The base peak for [CuTHC-H]$^+$ was found to be *m/z* 320.0829/322.0813 for ^{63}Cu and ^{65}Cu respectively, with *m/z* 313.2164 and 338.0936/340.0918 being the 2nd and 3rd most intense product ions, respectively. A summary of product ion assignments and proposed structures for [CuTHC-H]$^+$ fragmentation is given in Figure S1. For [CuCBD-H]$^+$, the base peak at 20 V HCD was observed to be *m/z* 252.0204/254.0188, followed by 308.0831/310.0814 and 266.0364/268.0345. A summary of product ion assignments and proposed structures for [CuCBD-H]$^+$ is given in Figure S2. While none of the product ion signals observed are completely exclusive to either THC or CBD, there is a very large difference in the relative intensities of the dominant fragments for [CuTHC-H]$^+$ and [CuCBD-H]$^+$, suggesting the potential for

differentiation by direct mass spectrometry. The isotope ratio for ^{63}Cu to ^{65}Cu is 69 % to 31 %,[48] versus 51 % to 49 % for ^{107}Ag and ^{109}Ag,[48] a further benefit of using ^{63}Cu cationization for cannabinoid quantitation.

Lithium Adducts. The second most intense metal ion adducts observed by ESI-HRMS were $[LiTHC]^+$ and $[LiCBD]^+$. While lithium should give more sensitive transitions because its adduct parent ions are less distributed across multiple isotopes when compared to Ag or Cu (^6Li ~8 % and ^7Li ~92 %)[48], lithium adducts were not as intense as the $[M+H]^+$ peak (*m/z* 315.1) for THC, implying that Li adduct (*m/z* 321.1) formation is not very favourable for THC (Figure 3A). This is supported by computational results summarized in Tables S9-S11, where the lithium cannabinoid adducts show less thermodynamic favourability when compared to either Ag or Cu based adducts. However, for CBD, the lithium adduct was more intense than the $[M+H]^+$ peak. Both the π bond and the aromatic hydroxyl group in cannabinoids donate electron density to Li^+, stabilizing the complex. Further, it was observed that lithium forms hydrated adducts with THC, where the H_2O oxygen will likely act as the 3rd coordinating atom to provide a stable complex. Product ions for $[LiTHC]^+$ and $[LiCBD]^+$ did not differ significantly at any observed collision energy. At 30 V HCD energy, the primary product ions for both $[LiTHC]^+$ and $[LiCBD]^+$ are *m/z* 237.1465, 255.1567, 199.1307, and 217.1410, with 237.1465 being the base peak and 217.1410 being the least intense (Figure 3B). Tentative product assignments based on HRMS and isotopic peaks are presented in Figure S3. The lack of differential fragmentation for lithium adducts can be explained by the tight association of lithium to the cannabinoid hydroxyl groups, giving similar fragmentation for THC and CBD, much like either cannabinoid without cationization.[49]

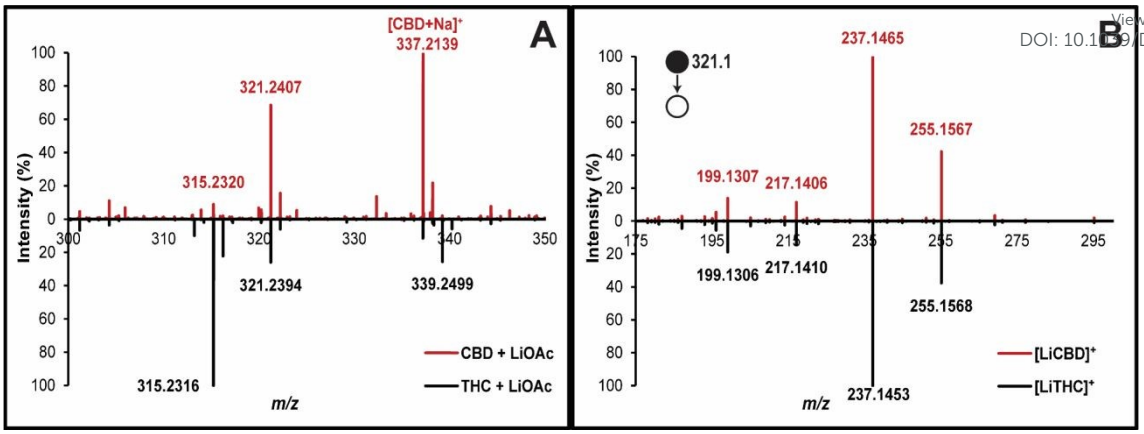

Figure 3. (A) Methanolic cannabinoid + LiOAc full scan spectra. $[LiTHC]^+$ adducts were observed at *m/z* 321.2394/322.2435, and their respective hydrated adducts were observed at +18 *m/z* to the corresponding peaks. $[LiCBD]^+$ adducts were also observed at *m/z* 321.2407/322.2431, however hydrated adducts were less intense. (B) Product ion spectra of $[^7LiTHC]^+$ and $[^7LiCBD]^+$ adducts at 30 V HCD, 120 000 Orbitrap resolution. Precursor ion $[^7LiCannabinoid]^+$, *m/z* 321.1. No meaningful differentiation is observed in the product ion spectra.

Tin and Palladium Adducts. Neither palladium or tin adducts of THC and CBD were observed in great intensity, with palladium adducts only observed for CBD, and tin adducts only for THC. These adducts were confirmed by HRMS, however the $[SnTHC]^+$ adducts were distributed across the ten stable tin isotopes, and in such low intensity that HRMS product ion spectra were unreliable. While palladium also suffers from a large isotopic distribution (6 stable isotopes)[48], $[PdCBD-H]^+$ formed very similar product ions to $[AgCBD]^+$, expected because of their similarity in polarizability, electronegativity, and mass. For $[^{106}PdCBD-H]^+$ at 20 V HCD, we observed that *m/z* 417.1036 was the base peak, corresponding to the loss of H_2 from the precursor ion. Similar to other observations for $[AgCBD]^+$,[19,21] *m/z* 231.1381, and 313.2163 were observed in significant intensity for $[^{106}PdCBD-H]^+$ fragment ions, shown in Figure S4.

Copper Cannabinoid MS/MS Selectivity. MS/MS selectivity for copper cannabinoid adducts was evaluated using both ESI and PS-MS. For each ionization method, two calibration series were prepared, one containing only THC and ISTD and the other containing only CBD and ISTD. Selectivity was assessed by dividing the calibration slope for the MRM of interest for the target cannabinoid

by the calibration slope obtained in the absence of cannabinoid. For example, the selectivity of the CBD MRM was evaluated by dividing the resulting slope from the CBD calibration series by the THC calibration slope. Results of all selectivity studies are summarized in Table S12, and sample calibration curves for ESI selectivity are given in Figure S5. Selectivity for PS-MS MRMs, given in Figure 4, was evaluated in a 3:1 acetonitrile/water matrix, as described above. For $[CuCBD]^+$, the *m/z* 377.1→231.1 MRM was observed to have 2% interference from THC (Figure 4A), whereas $[CuTHC+MeOH-H]^+$ (Figure 4B) was observed to have negligible (not differentiable from noise) interference by CBD. The reported 2% interference by THC for the *m/z* 377.1→231.1 transition is attributed to noise over the course of the run, with 20% error in the slope for the THC calibration and an r^2 of 0.8 as compared to 1% error in slope and 0.999 r^2 for the CBD calibration. High resolution spectra for the $[CuTHC+MeOH-H]^+$ and $[CuCBD]^+$ precursor are given in Figure S6.

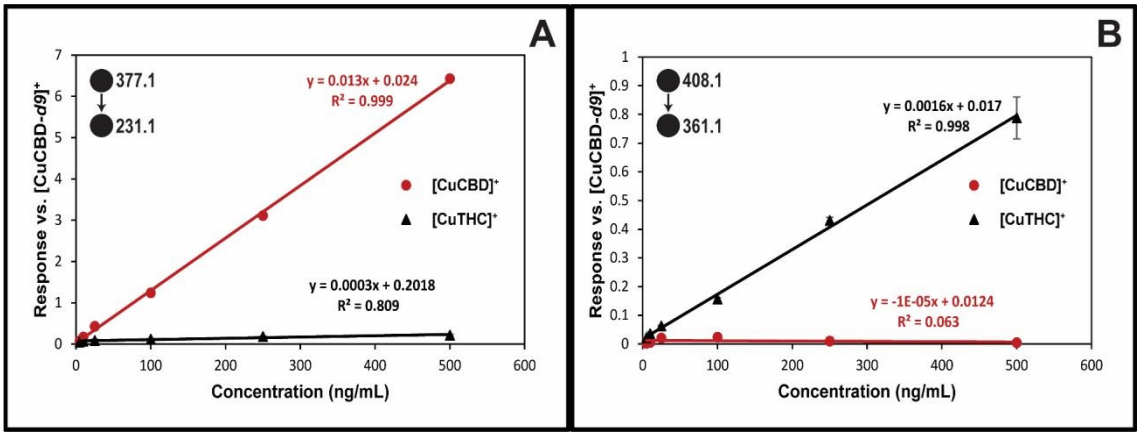

Figure 4. Calibration selectivity plots for THC and CBD obtained using copper cationization with PS-MS in acetonitrile/water matrix. Two calibration series are shown in each plot using the same MRM: one with varying concentrations of CBD (red lines, circles) and one with varying concentrations of THC (black lines, triangles). Error bars represent ± 1 standard deviation. (A) Selectivity plot for $[CuCBD]^+$ (MRM *m/z* 377.1→231.1). A steeper slope indicates greater response for the analyte of interest. (B) Selectivity plot for $[CuTHC+MeOH-H]^+$, (MRM *m/z* 408→361). Maximal response for the cannabinoid of interest is observed in both plots, whereas minimal response is observed for the absent analyte.

View Article Online
DOI: 10.1039/D5AN01073J

ESI selectivity was evaluated in methanolic standards, as acetonitrile-based standards complex any available copper thus preventing quantitation of copper adducts. For $[CuCBD]^+$, *m/z* 377.1→231.1, was observed to have <1% interference by THC and an LLOD of 0.15 ng/mL (Figure S5A), indicating that CBD can be effectively discriminated from THC using copper cationization. For THC, the transition which was both sensitive and semi-selective was *m/z* 376.1→361.1 (Figure S5B), with 6% interference by CBD and an LLOD of 10 ng/mL. Other MRMs, such as *m/z* 377.1→313.1 had negligible (<1 %) interference, but an inferior LLOD of 100 ng/mL. The most sensitive MRM, *m/z* *m/z* 376.1→320.1 exhibited 33 % interference by CBD, and is not useful for selectivity. However, it could be combined with ion mobility to increase both sensitivity and selectivity of copper THC adducts.

The lack of sensitivity for THC with ESI in methanolic standards is likely due to the lack of free rotation around the ring-ring single bond in THC, creating less favourable geometry for the complexation. Figure S7 illustrates a comparison of the computationally optimized geometries for both THC and CBD copper adducts. This is reflected by their precursor ion intensities, for which THC is 7x less intense than CBD at an equivalent concentration. Overall, this shows promising discrimination of CBD from THC by copper cationization with ESI, however analytical sensitivity needs to be optimized for use in biofluids. For regulatory use, the concentration of THC may be no more than 0.3 % in CBD oils.[4] As most CBD oils typically range in the high mg/mL region, copper cationization with ESI could serve as a viable direct analytical method to quantify both CBD and THC without significant interference for regulatory purposes.

PS-MS and Design of Experiment Optimization

Copper ion impregnated PS-MS paper strips were prepared by soaking the papers in solutions of methanolic CuCl. To optimize signal intensity, two DoE central composite studies were conducted using a total of 26 paper strips per sample matrix. The resulting DoE response surface for methanolic standards has a cubic fit, given in Figure 5a. From this, the optimized concentration and soak time for the PS-MS measurement of methanolic standards was determined to be 200 µg/mL CuCl in MeOH for 30 minutes. For saliva matrix standards, the

optimized concentration and soak time from a quadratic fit was 600 µg/mL CuCl in MeOH for 25 minutes (Figure 5b).

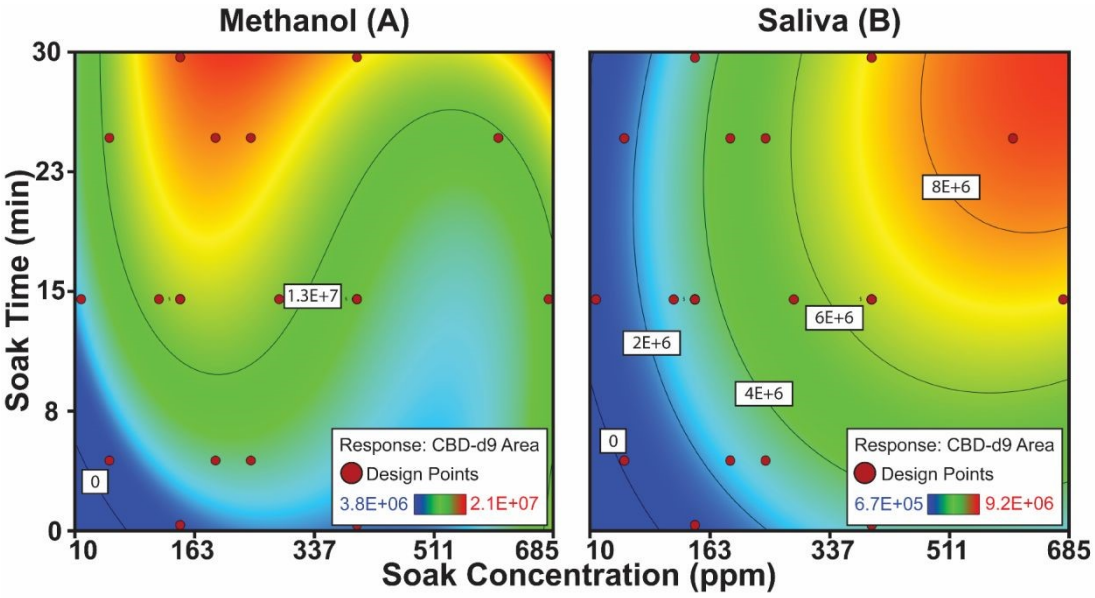

Figure 5. Sample DoE response contour for CBD-d_9 (*m/z* 385.1→317.1) in MeOH (A) and Saliva (B). Methanol: sequential fit *p<0.0001* lack of fit *p=0.2535*, cubic fit. Saliva: sequential fit *p<0.0001* lack of fit *p=0.9829*, quadratic fit.

Using optimized copper impregnated paper strips, PS-MS calibrations for methanolic, acetonitrile/water, and saliva sample matrices with PS-MS were prepared with combined standards of THC, CBD, with CBD-d_9 as internal standard. Proposed ion structures for these quantitative MRMs are illustrated in Figure 6. Calibration verifications were performed using prepared standards containing individual cannabinoids and ISTD. The resulting calibration curves are given in Figure S8 for methanolic standards, Figure S9 for acetonitrile/water matrix, and Figure S10 for saliva matrix. For PS-MS, the $[CuTHC+MeOH-H]^+$ precursor (*m/z* 408.1→361.1 MRM) was the most intense and was used for calibration, whereas for CBD, the $[CuCBD]^+$ (*m/z* 377.1→231.1 MRM) precursor was optimal.

View Article Online
DOI: 10.1039/D5AN01073J

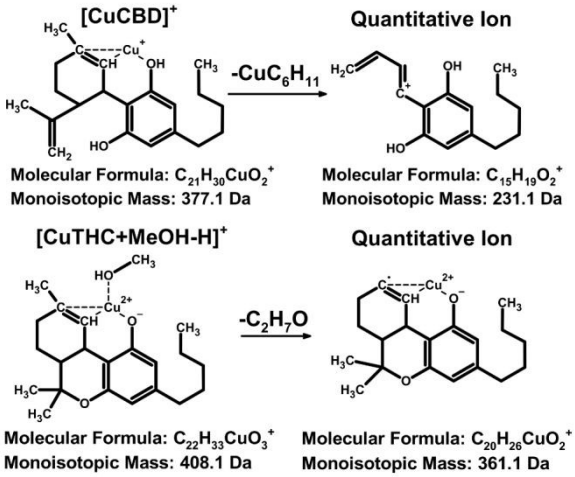

Figure 6. Proposed ion structures for the quantitative MRMs employed for copper cationization PS-MS.

Methanolic standard calibrations, shown in Figure S8 provided good analytical performance in the case of CBD, where the LLOD is calculated as 10 ng/mL (Table 1). However, for THC, the LLOD is 20 ng/mL. Calibration verification standards measured at 50 and 300 ng/mL were within 20 % bias, however at 10 ng/mL (below LLOD) a 30-70% bias from the expected concentration was observed. Calibration verification results are summarized in Table S13. Samples prepared in acetonitrile/water matrix had far better analytical figures of merit, with the LLOD for CBD and THC being 0.6 and 0.75 ng/mL, respectively. We hypothesize that the higher LLOD for methanolic standards is due to less favourable complexation conditions when spotted on the CuCl impregnated paper. Acetonitrile and water used both in the 3:1 ACN/H_2O and saliva matrices have a far greater solubility for CuCl, allowing more copper ions to be dissolved from the paper and complex with the cannabinoids as compared to methanolic solutions. This is supported by the calibration data in Figures S7 and S8, illustrating better low concentration linearity when compared to methanolic calibrations in Figure S8. The copper impregnated PS-MS papers exhibited no degradation in analytical performance over a three-day period as shown in Figure S11.

View Article Online
DOI: 10.1039/D5AN01073J

Table 1. Analytical figures of merit and calibration information for THC (*m/z* 408.1→361.1) and CBD (*m/z* 377.1→231.1) measurement using copper cationization PS-MS by sample measurement matrix.

Matrix	Cannabinoid	Slope	Intercept	R^2	LLOD* (ng/mL)	LLOQ** (ng/mL)
MeOH	THC	0.0021	0.032	0.991	20	67
	CBD	0.0158	0.151	0.996	10	33
3:1 ACN:H_2O	THC	0.0019	0.061	0.997	0.75	2.50
	CBD	0.0141	0.191	0.999	0.61	2.03
Saliva	THC	0.0019	0.257	0.998	1.9	6.3
	CBD	0.0106	0.743	0.997	1.3	4.3

*LLOD is estimated by determining signal to noise with the formula (Avg $Signal_{Calibrator}$ - Avg $Signal_{Blank}$)/Std. Dev_{Blank}, and using the lowest calibrator with signal to noise >3 to extrapolate back to the concentration with a signal-to-noise of 3.[50]
**Lower Limit of Quantitation (LLOQ) calculated as 3.33x LLOD.

Analytical performance was acceptable in saliva matrix, even with a 3:1 protein crash diluting the initial cannabinoid concentrations by 4x. LLODs, given in Table 1, were 1.3 ng/mL for CBD, and 1.9 ng/mL for THC . Calibration curves for the saliva matrix are shown in Figure S10. Calibration verification samples, summarized in Table S13, were all within 20% bias and were randomly distributed indicating no systematic interference by either cannabinoid. For regulatory testing, SAMHSA recommends a cutoff of 2 ng/mL for THC in saliva, suggesting that the on-paper copper cationization PS-MS method presented provides sufficient sensitivity for regulatory testing,[5] while requiring only one minute of measurement. To our knowledge, this strategy is the most sensitive direct mass spectrometry method reported to date for quantifying CBD and THC, providing acceptable selectivity without any chromatographic separation.

CONCLUSIONS

Computational chemistry and DoE are useful methods which can accelerate the development and optimization of new analytical methods. We exemplify this through the development of on-paper copper cationization for the direct PS-MS measurement of cannabinoids at trace levels in a one-minute measurement. PS-MS paper strips impregnated with copper chloride allow cationization to occur on the sample strip simplifying analytical workflow, and from preliminary studies are stable for multiple days after drying. The presented PS-

MS methods are sufficient to obtain LLODs of <2 ng/mL for THC and CBD, with calibration linearity over three orders of magnitude in saliva, meeting regulatory detection limits and suggesting potential for use as a rapid one-minute screening method with further validation of sensitivity and robustness.[5] Employing miniature or portable mass spectrometer systems with our approach could provide an alternative to conventional immunoassay-based roadside testing. Copper cannabinoid cationization provides excellent selectivity (<1% interference) between THC and CBD using direct tandem mass spectrometry without the need for chromatographic separation. The use of other metal cationization reagents, such as lithium, could be explored for determining total cannabinoid concentration due to the similarity of fragmentation patterns for THC and CBD lithium adducts. Literature and computational results suggest that copper (I) complexation is more thermodynamically favourable than silver (I) with both alkenes and alkynes.[46] Therefore, compounds which enjoy ionization enhancement from silver (I) could be revisited with copper (I) to test for increased analytical performance due to the better isotopic ratio associated with copper. We present one such use of copper cationization with PS-MS for selectively quantifying the isobaric cannabinoids THC and CBD at trace levels. Future work will involve method optimization in other biofluids and investigation using ion mobility spectrometry with copper cationization for the analysis of other isobaric and psychoactive cannabinoids in commercial products. The methods presented herein could be explored to simplify and accelerate regulatory testing of CBD and THC in both saliva and in cannabis extract products.

AUTHOR CONTRIBUTIONS

Jindar N.S. Sboto: conceptualization, methodology, validation, formal analysis, investigation, writing – original draft preparation, writing – reviewing and editing. Chris G. Gill: conceptualization, resources, supervision, writing – reviewing and editing, funding acquisition.

CONFLICTS OF INTEREST

There are no conflicts to declare.

View Article Online
DOI: 10.1039/D5AN01073J

DATA AVAILABILITY STATEMENT

Files for the density functional theory computations are openly available free of charge using the creative commons license CC BY-NC-SA 4.0 at the Vancouver Island University database entry: https://doi.org/10.5683/SP3/VQ3QNQ. Experimental data have been included with the supplementary information.

SUPPLEMENTARY INFORMATION

The supplementary information is available free of charge with this document. The supplementary information summarizes additional instrumental parameters, density functional theory results, proposed fragmentation diagrams, calibration curves, and stability results for copper cationization of cannabinoids.

ACKNOWLEDGMENTS

This research was funded by a Natural Science and Engineering Research Council (NSERC) Discovery Grant (RGPIN-2021-02981) and infrastructure provided by the Canadian Foundation for Innovation: John R. Evans Leaders Fund & British Columbia Knowledge Development Fund (CFI 40274). J.N.S. Sboto was supported in part by the NSERC USRA program, a British Columbia Graduate Scholarship, and the Armin Saatchi Chemistry Award. The authors gratefully acknowledge Thermo Fisher Scientific for providing the instruments used in this study and for ongoing technical support, and thank both the University of Victoria and Vancouver Island University for their support of our research. This research was enabled in part by support from the BC DRI Group, Compute Ontario, and the Digital Research Alliance of Canada (alliancecan.ca). Special thanks are extended to Mr. Lucas Abruzzi for use of his in-house developed paper spray source, Dr. Erik Krogh for his advice on design of experiment, Dr. Heather Wiebe and the VIU modelling lab for their assistance in learning computational chemistry, and Dr. Christian Ieritano for his insights on cannabinoid metal adduct complexation.

View Article Online
DOI: 10.1039/D5AN01073J

REFERENCES

(1) Wang, Q.; Qin, Z.; Xing, X.; Zhu, H.; Jia, Z. Prevalence of Cannabis Use around the World: A Systematic Review and Meta-Analysis, 2000–2024. *China CDC Wkly.* **2024**, *6* (25), 597–604. https://doi.org/10.46234/ccdcw2024.116.

(2) Sheikh, N. K.; Dua, A. Cannabinoids. In *StatPearls*; StatPearls Publishing: Treasure Island (FL), 2025.

(3) National Academies of Sciences, E.; Division, H. and M.; Practice, B. on P. H. and P. H.; Agenda, C. on the H. E. of M. A. E. R. and R. Therapeutic Effects of Cannabis and Cannabinoids. In *The Health Effects of Cannabis and Cannabinoids: The Current State of Evidence and Recommendations for Research*; National Academies Press (US), 2017.

(4) DeCarlo, S.; Weaver, M. Keeping the High out of Hemp: Global THC Standards. **2023**.

(5) Federal Register/Vol. 76, No. 204/Friday, October 21, 2011/Rules and Regulations: (722922011-001), 2011. https://doi.org/10.1037/e722922011-001.

(6) Brubacher Jeffrey R.; Chan Herbert; Erdelyi Shannon; Staples John A.; Asbridge Mark; Mann Robert E. Cannabis Legalization and Detection of Tetrahydrocannabinol in Injured Drivers. *N. Engl. J. Med.* **2022**, *386* (2), 148–156. https://doi.org/10.1056/NEJMsa2109371.

(7) Blencowe, T.; Pehrsson, A.; Lillsunde, P.; Vimpari, K.; Houwing, S.; Smink, B.; Mathijssen, R.; Van der Linden, T.; Legrand, S.-A.; Pil, K.; Verstraete, A. An Analytical Evaluation of Eight On-Site Oral Fluid Drug Screening Devices Using Laboratory Confirmation Results from Oral Fluid. *Forensic Sci. Int.* **2011**, *208* (1), 173–179. https://doi.org/10.1016/j.forsciint.2010.11.026.

(8) Hambidge, T.; Nash, R.; Corless, S.; Sanatcumar, P.; Bowdery, P.; Griffin, J.; Sears, P.; J. Hopley, C. Validated LC-MS/MS Methodology for the Quantification of CBD, Trace Level THCA and UK Controlled Cannabinoids (Δ 9 -THC, Δ 8 -THC, CBN and THCV) in Food Samples. *Anal. Methods* **2025**, *17* (6), 1306–1316. https://doi.org/10.1039/D4AY01946F.

(9) Borden, S. A.; Saatchi, A.; Vandergrift, G. W.; Palaty, J.; Lysyshyn, M.; Gill, C. G. A New Quantitative Drug Checking Technology for Harm Reduction: Pilot Study in Vancouver, Canada Using Paper Spray Mass Spectrometry. *Drug Alcohol Rev.* **2022**, *41* (2), 410–418. https://doi.org/10.1111/dar.13370.

(10) Espy, R. D.; Teunissen, S. F.; Manicke, N. E.; Ren, Y.; Ouyang, Z.; van Asten, A.; Cooks, R. G. Paper Spray and Extraction Spray Mass Spectrometry for the Direct and Simultaneous Quantification of Eight Drugs of Abuse in Whole Blood. *Anal. Chem.* **2014**, *86* (15), 7712–7718. https://doi.org/10.1021/ac5016408.

(11) Frey, B. S.; Damon, D. E.; Badu-Tawiah, A. K. Emerging Trends in Paper Spray Mass Spectrometry: Microsampling, Storage, Direct Analysis and Applications. *Mass Spectrom. Rev.* **2020**, *39* (4), 336–370. https://doi.org/10.1002/mas.21601.

(12) Su, Y.; Wang, H.; Liu, J.; Wei, P.; Cooks, R. G.; Ouyang, Z. Quantitative Paper Spray Mass Spectrometry Analysis of Drugs of Abuse. *Analyst* **2013**, *138* (16), 4443–4447. https://doi.org/10.1039/C3AN00934C.

(13) Banerjee, S.; Mazumdar, S. Electrospray Ionization Mass Spectrometry: A Technique to Access the Information beyond the Molecular Weight of the Analyte. *Int. J. Anal. Chem.* **2012**, *2012*, 282574. https://doi.org/10.1155/2012/282574.

(14) Zimmerman-Federle, H.; Ren, G.; Dowling, S.; Warren, C.; Rusyniak, D.; Avera, R.; Manicke, N. E. Plasma Drug Screening Using Paper Spray Mass Spectrometry with Integrated Solid Phase Extraction. *Drug Test. Anal.* **2025**, *17* (1), 138–151. https://doi.org/10.1002/dta.3687.

(15) Ren, G.; Bills, B. J.; Manicke, N. E. Analysis of Drugs in Whole Blood by Paper Spray Mass Spectrometry with Integrated Solid-Phase Extraction. *Anal. Chem.* **2025**, *97* (26), 14004–14012. https://doi.org/10.1021/acs.analchem.5c02394.

(16) Bills, B.; Manicke, N. Using Sesame Seed Oil to Preserve and Preconcentrate Cannabinoids for Paper Spray Mass Spectrometry. *J. Am. Soc. Mass Spectrom.* **2020**, *31* (3), 675–684. https://doi.org/10.1021/jasms.9b00113.

(17) Bills, B. J.; Kinkade, J.; Ren, G.; Manicke, N. E. The Impacts of Paper Properties on Matrix Effects during Paper Spray Mass Spectrometry Analysis of Prescription Drugs, Fentanyl and Synthetic Cannabinoids. *Forensic Chem.* **2018**, *11*, 15–22. https://doi.org/10.1016/j.forc.2018.08.002.

(18) Espy, R. D.; Teunissen, S. F.; Manicke, N. E.; Ren, Y.; Ouyang, Z.; van Asten, A.; Cooks, R. G. Paper Spray and Extraction Spray Mass Spectrometry for the Direct and Simultaneous Quantification of Eight Drugs of Abuse in Whole Blood. *Anal. Chem.* **2014**, *86* (15), 7712–7718. https://doi.org/10.1021/ac5016408.

(19) Ieritano, C.; Thomas, P.; Hopkins, W. S. Argentination: A Silver Bullet for Cannabinoid Separation by Differential Mobility Spectrometry. *Anal. Chem.* **2023**, *95* (22), 8668–8678. https://doi.org/10.1021/acs.analchem.3c01241.

(20) Satterfield, M.; Brodbelt, J. S. Enhanced Detection of Flavonoids by Metal Complexation and Electrospray Ionization Mass Spectrometry. *Anal. Chem.* **2000**, *72* (24), 5898–5906. https://doi.org/10.1021/ac0007985.

(21) Huang, S.; Claassen, F. W.; van Beek, T. A.; Chen, B.; Zeng, J.; Zuilhof, H.; Salentijn, G. IJ. Rapid Distinction and Semiquantitative Analysis of THC and CBD by Silver-Impregnated Paper Spray Mass Spectrometry. *Anal. Chem.* **2021**, *93* (8), 3794–3802. https://doi.org/10.1021/acs.analchem.0c04270.

(22) Couch, A. N.; Lanza, J. M.; Zall, C. M.; Davidson, J. T. Differentiation of Δ9-THC and CBD Using Silver-Ligand Ion Complexation and Electrospray Ionization Tandem Mass Spectrometry (ESI-MS/MS). *J. Am. Soc. Mass Spectrom.* **2024**, *35* (7), 1413–1421. https://doi.org/10.1021/jasms.3c00452.

(23) Couch, A. N.; Lanza, J. M.; Zall, C. M.; Davidson, J. T. Identification of Marijuana Using Silver-Phosphine Ion Complexation and a Semi-Quantitative 1 % Decision-Point Assay. *Talanta Open* **2024**, *10*, 100359. https://doi.org/10.1016/j.talo.2024.100359.

(24) Borden, S. A.; Saatchi, A.; Palaty, J.; Gill, C. G. A Direct Mass Spectrometry Method for Cannabinoid Quantitation in Urine and Oral Fluid Utilizing Reactive Paper Spray Ionization. *Analyst* **2022**, *147* (13), 3109–3117. https://doi.org/10.1039/D2AN00743F.

(25) Ma, Q.; Bai, H.; Li, W.; Wang, C.; Cooks, R. G.; Ouyang, Z. Rapid Analysis of Synthetic Cannabinoids Using a Miniature Mass Spectrometer

with Ambient Ionization Capability. *Talanta* **2015**, *142*, 190–196. https://doi.org/10.1016/j.talanta.2015.04.044.

(26) Chen, C.-H.; Lin, Z.; Tian, R.; Shi, R.; Cooks, R. G.; Ouyang, Z. Real-Time Sample Analysis Using a Sampling Probe and Miniature Mass Spectrometer. *Anal. Chem.* **2015**, *87* (17), 8867–8873. https://doi.org/10.1021/acs.analchem.5b01943.

(27) Grade, H.; Cooks, R. G. Secondary Ion Mass Spectrometry. Cationization of Organic Molecules with Metals. *J. Am. Chem. Soc.* **1978**, *100* (18), 5615–5621. https://doi.org/10.1021/ja00486a006.

(28) Thorsteinsdóttir, U. A.; Thorsteinsdóttir, M. Design of Experiments for Development and Optimization of a Liquid Chromatography Coupled to Tandem Mass Spectrometry Bioanalytical Assay. *J. Mass Spectrom.* **2021**, *56* (9), e4727. https://doi.org/10.1002/jms.4727.

(29) Frisch, M. J.; Trucks, G. W.; Schlegel, H. B.; Scuseria, G. E.; Robb, M. A.; Cheeseman, J. R.; Scalmani, G.; Barone, V.; Petersson, G. A.; Nakatsuji, H.; Li, X.; Caricato, M.; Marenich, A. V.; Bloino, J.; Janesko, B. G.; Gomperts, R.; Mennucci, B.; Hratchian, H. P.; Ortiz, J. V.; Izmaylov, A. F.; Sonnenberg, J. L.; Williams; Ding, F.; Lipparini, F.; Egidi, F.; Goings, J.; Peng, B.; Petrone, A.; Henderson, T.; Ranasinghe, D.; Zakrzewski, V. G.; Gao, J.; Rega, N.; Zheng, G.; Liang, W.; Hada, M.; Ehara, M.; Toyota, K.; Fukuda, R.; Hasegawa, J.; Ishida, M.; Nakajima, T.; Honda, Y.; Kitao, O.; Nakai, H.; Vreven, T.; Throssell, K.; Montgomery Jr., J. A.; Peralta, J. E.; Ogliaro, F.; Bearpark, M. J.; Heyd, J. J.; Brothers, E. N.; Kudin, K. N.; Staroverov, V. N.; Keith, T. A.; Kobayashi, R.; Normand, J.; Raghavachari, K.; Rendell, A. P.; Burant, J. C.; Iyengar, S. S.; Tomasi, J.; Cossi, M.; Millam, J. M.; Klene, M.; Adamo, C.; Cammi, R.; Ochterski, J. W.; Martin, R. L.; Morokuma, K.; Farkas, O.; Foresman, J. B.; Fox, D. J. Gaussian 16 Rev. C.01, 2016.

(30) Dennington, R.; Keith, T. A.; Millam, J. M. GaussView Version 6, 2019.

(31) Chai, J.-D.; Head-Gordon, M. Long-Range Corrected Hybrid Density Functionals with Damped Atom–Atom Dispersion Corrections. *Phys. Chem. Chem. Phys.* **2008**, *10* (44), 6615–6620. https://doi.org/10.1039/B810189B.

(32) Chai, J.-D.; Head-Gordon, M. Systematic Optimization of Long-Range Corrected Hybrid Density Functionals. *J. Chem. Phys.* **2008**, *128* (8), 084106. https://doi.org/10.1063/1.2834918.

(33) Andrae, D.; Häußermann, U.; Dolg, M.; Stoll, H.; Preuß, H. Energy-Adjustedab Initio Pseudopotentials for the Second and Third Row Transition Elements. *Theor Chim Acta* **1990**, *77*, 123–141. https://doi.org/10.1007/bf01114537.

(34) Feller, D. The Role of Databases in Support of Computational Chemistry Calculations. *J Comput Chem* **1996**, *17*, 1571–1586. https://doi.org/10.1002/(SICI)1096-987X(199610)17:13%253C1571::AID-JCC9%253E3.0.CO;2-P.

(35) Metz, B.; Stoll, H.; Dolg, M. Small-Core Multiconfiguration-Dirac-Hartree-Fock-Adjusted Pseudopotentials for Post-d Main Group Elements: Application to PbH and PbO. *J Chem Phys* **2000**, *113*, 2563–2569. https://doi.org/10.1063/1.1305880.

(36) Pritchard, B. P.; Altarawy, D.; Didier, B.; Gibson, T. D.; Windus, T. L. New Basis Set Exchange: An Open, Up-to-Date Resource for the Molecular

Sciences Community. *J. Chem. Inf. Model.* **2019**, *59* (11), 4814–4820. https://doi.org/10.1021/acs.jcim.9b00725.

(37) Rappoport, D.; Furche, F. Property-Optimized Gaussian Basis Sets for Molecular Response Calculations. *J Chem Phys* **2010**, *133*, 134105. https://doi.org/10.1063/1.3484283.

(38) Schuchardt, K. L.; Didier, B. T.; Elsethagen, T.; Sun, L.; Gurumoorthi, V.; Chase, J.; Li, J.; Windus, T. L. Basis Set Exchange: A Community Database for Computational Sciences. *J Chem Inf Model* **2007**, *47*, 1045–1052. https://doi.org/10.1021/ci600510j.

(39) Weigend, F.; Ahlrichs, R. Balanced Basis Sets of Split Valence, Triple Zeta Valence and Quadruple Zeta Valence Quality for H to Rn: Design and Assessment of Accuracy. *Phys Chem Chem Phys* **2005**, *7*, 3297. https://doi.org/10.1039/b508541a.

(40) Ho, J.; Klamt, A.; Coote, M. L. Comment on the Correct Use of Continuum Solvent Models. *J. Phys. Chem. A* **2010**, *114* (51), 13442–13444. https://doi.org/10.1021/jp107136j.

(41) Hay, P. J.; Wadt, W. R. Ab Initio Effective Core Potentials for Molecular Calculations. Potentials for K to Au Including the Outermost Core Orbitals. *J Chem Phys* **1985**, *82*, 299–310. https://doi.org/10.1063/1.448975.

(42) Dunning, T. H.; Hay, P. J. Gaussian Basis Sets for Molecular Calculations. In *Methods of Electronic Structure Theory*; Schaefer, H. F., Ed.; Modern Theoretical Chemistry; Springer, 1977; Vol. 3, pp 1–27. https://doi.org/10.1007/978-1-4757-0887-5.

(43) Pereira, I.; Sboto, J. N. S.; Robinson, J. L.; Gill, C. G. Paper Spray Mass Spectrometry Combined with Machine Learning as a Rapid Diagnostic for Chronic Kidney Disease. *Analyst* **2024**, *149* (9), 2600–2608. https://doi.org/10.1039/D4AN00099D.

(44) Stat-Ease® 360 Software. www.statease.com.

(45) Abruzzi, L. R.; Laxton, J.-C.; Zarkovic, T. M.; Gill, C. G. Internal Standard Utilization Strategies for Quantitative Paper Spray Mass Spectrometry. *J. Am. Soc. Mass Spectrom.* **2025**, *36* (5), 1167–1174. https://doi.org/10.1021/jasms.5c00036.

(46) Mehara, J.; Watson, B. T.; Noonikara-Poyil, A.; Zacharias, A. O.; Roithová, J.; Rasika Dias, H. V. Binding Interactions in Copper, Silver and Gold π-Complexes. *Chem. Weinh. Bergstr. Ger.* **2022**, *28* (13), e202103984. https://doi.org/10.1002/chem.202103984.

(47) Goodgame, D. M. L.; Goodgame, M.; Canham, G. W. R. Reversible Oxidation of Copper(I) Iodide in the Presence of Imidazole. *Nature* **1969**, *222* (5196), 866–866. https://doi.org/10.1038/222866a0.

(48) Atomic Masses and Isotopic Composition of the Elements. In *CRC Handbook of Chemistry and Physics*; CRC Press, 2025.

(49) Mahmoud, R.; Khajavinia, A.; Barzegar, S.; Purves, R. W.; Laprairie, R. B.; El-Aneed, A. Establishment of a Mass Spectrometric Fingerprint of the Most Common Phytocannabinoids in Electrospray Ionization in Positive Ion Mode. *Rapid Commun. Mass Spectrom.* **2025**, *39* (4), e9952. https://doi.org/10.1002/rcm.9952.

(50) Vandergrift, G. W.; Hessels, A. J.; Palaty, J.; Krogh, E. T.; Gill, C. G. Paper Spray Mass Spectrometry for the Direct, Semi-Quantitative Measurement of Fentanyl and Norfentanyl in Complex Matrices. *Clin.*

Biochem. **2018**, *54*, 106–111.
https://doi.org/10.1016/j.clinbiochem.2018.02.005.

View Article Online
DOI: 10.1039/D5AN01073J

View Article Online
DOI: 10.1039/D5AN01073J

DATA AVAILABILITY STATEMENT

Files for the density functional theory computations are openly available free of charge using the creative commons license CC BY-NC-SA 4.0 at the Vancouver Island University database entry: https://doi.org/10.5683/SP3/VQ3QNQ. Experimental data have been included with the supplementary information.